CrystEngComm

RSC Publishing

COMMUNICATION

View Article Online
View Journal | View Issue

Chiral porous metal–organic frameworks from chiral building units with different metrics†

Cite this: *CrystEngComm*, 2013, **15**, 10161

Received 10th August 2013,
Accepted 4th October 2013

DOI: 10.1039/c3ce41586d

www.rsc.org/crystengcomm

Qiaowei Li,[ab] Sung Min Shin,[c] Dohyun Moon,[d] Kyung Seok Jeong[c] and Nakcheol Jeong*[c]

Two chiral MOFs from the common $Zn_4O(COO)_6$ SBUs and the congeners of chiral ligands were synthesized and characterized. The overall structures are differentiated by the ligand dimensions. These MOFs obtained from the flexible enantiopure struts exhibited severe chirality attenuation during the assembly.

Metal–organic frameworks[1] with chiral coverage domains,[2] where incoming molecules cover the surfaces of pores in MOFs, have attracted significant interest because of their potential for applications in enantioselective gas storage,[3] separation,[4] and catalysis.[5] Due to the weak, non-specific interactions between the guests and the frameworks, traditional MOFs show little selectivity towards guest molecules with similar sizes and shapes, such as racemics, on the surface. Thus, the value of MOFs has not often been proven in the areas of enantioselective catalysis and racemic separation, where a more sophisticated environment with different responses to racemics is essential. Of the several approaches devised to synthesize MOFs bearing specific chiral coverage domains, early examples involve the preparation of MOFs by linking readily available enantiopure struts with inorganic secondary building units (SBUs).[6] This approach not only provides the most reliable means for chiral MOF synthesis but also allows for further synthetic elaboration of chiral struts to impart desirable functionalities.

One intriguing advantage of MOFs is that the size and shape of the pores could be precisely tuned. Hitherto, most trials for the pore expansion of a given MOF have included an approach to employ a longer ligand, with the congener otherwise remaining the same. However, this approach has often failed to give a MOF with the same topology,[7] since the principles exhibited in one case are not necessarily applicable to other MOFs, even those closely related.[8] A new MOF structure is often formed by minimizing the void volume as the ligand length increases, *via* 1) the formation of an interpenetrated structure with the same skeleton,[9] or 2) generating completely different structures[10] while keeping the local SBU structure intact.

Herein, we report on two new MOF structures constructed from similar dicarboxylate ligands with different metrics and chirality attenuation during the self-assembly of these MOFs. Specifically, two organic chiral ligands, $1H_2$ and $2H_2$, bearing point chiralities,[9] were prepared for this study (Fig. 1a). Phenyl groups were employed to control the length of these ligands. Chiral MOFs built from these two flexible enantiopure struts and Zn(II) were synthesized, in which the common $Zn_4O(COO)_6$ SBUs were found. The SBUs further connect with the struts to provide single crystals of Zn-(+)-**1** with a layered structure and Zn-(+)-**2** packed with infinite 1D chains, which are fully characterized by single crystal X-ray diffraction and low pressure N_2 isotherm.‡

Specifically, colorless plate-shaped crystals of Zn-(+)-**1** and block crystals of Zn-(+)-**2** were obtained by solvothermal reactions of $1H_2$ with $Zn(NO_3)_2{\cdot}6H_2O$ and $2H_2$ with $Zn(OAc)_2$, respectively. Single crystal X-ray structural analysis reveals that the crystals of Zn-(+)-**1** and Zn-(+)-**2** belong to the chiral space groups $P1$ and $P2_12_12_1$, respectively (see ESI† for crystallographic details). Bulk purity of the samples was confirmed by powder X-ray diffractions, which show congruence of the peak positions in the experimental patterns and the simulated patterns from single x-ray data (Fig. S1†).

[a] *Department of Chemistry, Fudan University, 220 Handan Road, Shanghai 200433, China*
[b] *Center for Reticular Chemistry, Department of Chemistry and Biochemistry, University of California, Los Angeles, 607 East Charles E. Young Drive, Los Angeles, California 90095, USA*
[c] *Department of Chemistry, Korea University, Seoul, 136-701, Korea. E-mail: njeong@korea.ac.kr*
[d] *Beamline Division, Pohang Accelerator Laboratory/POSTECH, San-31 Hyoja-Dong, Nam-Gu, Pohang, Kyung Buk 790-784, Korea*

† Electronic supplementary information (ESI) available: Ligand preparation, MOF synthesis, TGA, PXRD, adsorption isotherms, and circular dichroism measurements of MOFs. CCDC 848661 and 834932. For ESI and crystallographic data in CIF or other electronic format see DOI: 10.1039/c3ce41586d

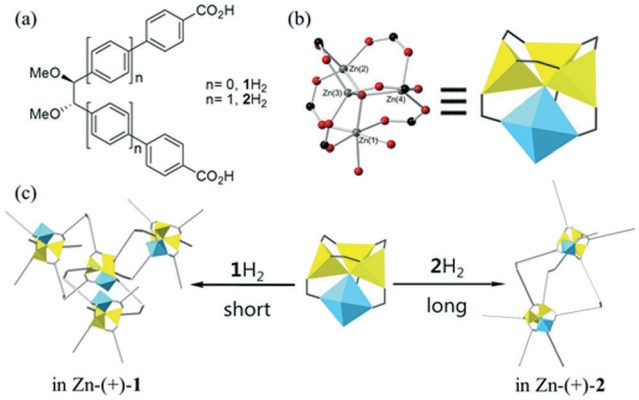

Fig. 1 (a) Ligands $\mathbf{1}H_2$ and $\mathbf{2}H_2$. (b) Common SBU found in Zn-(+)-**1** and Zn-(+)-**2**. (c) Asymmetric units of Zn-(+)-**1** and Zn-(+)-**2**.

The SBUs in both Zn-(+)-**1** and Zn-(+)-**2** are identical. They consist of a cluster of four zinc atoms connected to each other by μ-O. However, in contrast to the SBU found in MOF-5,[1a] one of the four zinc atoms in the SBU, Zn(1), is found to have octahedral coordination (denoted as a blue octahedron in Fig. 1b), while the other three remain tetrahedral (denoted as yellow tetrahedra). Zn(1) is coordinated with two oxygen atoms from solvent molecules, three oxygen atoms from carboxylates of three chiral ligands, and finally one oxygen atom residing at the center of the SBU.

Interestingly, even though the two crystals share the same SBU, the overall 3D structures of MOFs are differentiated by the ligand metrics, which further lead to the variation of the SBU connectivity (Fig. 1c). For Zn-(+)-**1**, which has a shorter ligand, the SBUs form a square by pairing two neighbouring SBUs and keeping the average dihedral angles of the two phenyl rings in each strut at approximately 60° (Fig. 2a). Each SBU is connected to three neighboring SBUs by six struts, creating a two-dimensional graphite topology network with an average edge length of 12 Å (Fig. 2a and b).

Graphite-like 2D sheets are further stacked to form an extended network. A view from the top of the layers of Zn-(+)-**1** reveals that the layers are packed in an eclipsed geometry, although every two neighboring layers are not crystallographically identical. In other words, if all four SBUs in the asymmetric unit of the structure are considered to be different in a strict sense, the layers are packed in the ABAB mode (as shown in red and blue in Fig. 2b). However, the packing can be described as AAA packing topology if the subtle differences between layers were neglected. The distance between every two layers is approximately 12 Å.

From the crystal structure of Zn-(+)-**1**, we can point out that two types of pores exist in the structure: (i) channels with 6 Å diameter exist along the centers of the hexagons, with all the stereogenic centers exposed to the channels; and (ii) small cages formed by a pair of bent struts and the two SBUs connecting them. To further demonstrate the porous nature of this MOF, nitrogen adsorption isotherm measurements (Fig. 2c) were performed on an evacuated sample of the acetone-exchanged Zn-(+)-**1** solid. The solvent-exchanged

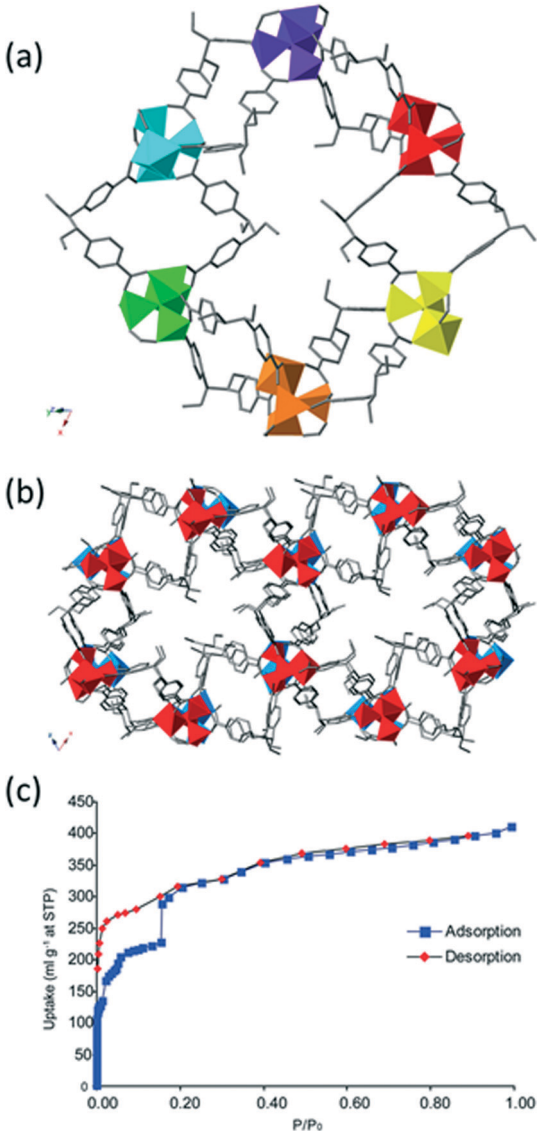

Fig. 2 (a) Top view of Zn-(+)-**1**. (b) Overlay of two layers of Zn-(+)-**1**. (c) N_2 gas adsorption and desorption data of Zn-(+)-**1** at 77 K.

solid shows a different PXRD pattern due to the possible inter-layer distance change during the solvent exchange process (Fig. S7†) but still keeps high crystallinity. Indeed, two-step gas adsorption behavior was observed for the adsorption, which indicates a microporous material with possible structural change. The reproducibility of the isotherm and the structural integrity of this MOF during the tests were confirmed by repeating the adsorption–desorption cycle three times. Significantly, all gas molecules can be removed, as observed in the desorption branch of the isotherm. A Langmuir surface area of 1050 $m^2\ g^{-1}$ and a BET surface area of 830 $m^2\ g^{-1}$ have been obtained from the adsorption branch. It is remarkable that Zn-(+)-**1**, a two-dimensional structure, exhibits porosity similar to that of three-dimensional MOF structures.

A hysteresis loop is observed in the nitrogen adsorption isotherm of Zn-(+)-**1**. Hysteresis loops in 77 K nitrogen isotherms closing at a relative pressure lower than 0.42 P/P_0

cannot be attributed to the capillary condensation of N_2 in the mesopores. Instead, the swelling of a non-rigid porous structure is the cause of the hysteresis, considering (i) the flexibility of the struts in the framework and (ii) the possible interlayer distance change in the two-dimensional structure under different conditions. We believe that when the relative pressure approaches 0.25 P/P_0 during the measurement, the structure swells, opening more space for nitrogen molecules until the material becomes saturated again after the relative pressure reaches 0.27 P/P_0. However, the desorption curve shows that all the N_2 molecules are removed in one step. The PXRD pattern of Zn-(+)-**1** after sorption test remains the same as that of the solvent-exchanged Zn-(+)-**1** (Fig. S7†), suggesting that the hysteresis has nothing to do with the structural collapse. The pore volume has been calculated with a D–R model to be 0.28 $cm^3\ g^{-1}$ using an adsorption curve and 0.46 $cm^3\ g^{-1}$ using a desorption curve. A similar gate effect was observed in the argon adsorption isotherm at 87 K on the same sample, with a lower gate pressure at around 0.16 P/P_0 (Fig. S5†). Furthermore, the hydrogen adsorption isotherm and carbon dioxide isotherm of Zn-(+)-**1** show that this MOF adsorbs 0.79 wt% H_2 at 1 atm, 77 K or 5.12 wt% CO_2 at 1 atm, 273 K (Fig. S6†).

For Zn-(+)-**2**, which is constructed from a longer ligand, $2H_2$, the increased space between two neighboring SBUs allows the connection of three ligands to form a pocket (Fig. 1c and 3a). In other words, for all three ligands, one end of each bidentate ligand holds the same SBU, and the other end binds the neighboring SBU in the same manner. These pockets are fused by sharing the inorganic SBUs to make a 1D chain running along the crystallographic *c*-axis. As a result, a one-dimensional rod with pockets having 16.4 Å distances between SBUs was obtained. From the top view, the rod is projected as sets of propellers with three blades, in which the dihedral angles are nearly 120°. The second set of the blades rotates by 60° from the first set to form a staggered arrangement, and the successive 60° rotation for the third set leads to overlapping with the first one (Fig. 3b).

Furthermore, necklace-like 1D rods are placed parallel to each other and packed to form a columnar bundle with grooves snugly fitted by the branches of neighboring rods. As a result, the BET measurements on Zn-(+)-**2** at 77 K show the nonporous nature of the material (with a calculated free solvent-accessible volume of only 3.0%).

These chiral MOFs are assumed to bear the chiral coverage domains since they are built from the enantiopure struts. However, the chiral bias, which the guest molecules might experience, does not seem to be substantial in these MOFs, as seen in the case of cyclodextrins.[11] Contrary to common sense, the chirality attenuation during the supramolecule formation—the mitigation of chirality bias instead of the amplification or preservation of that implanted on the component—is

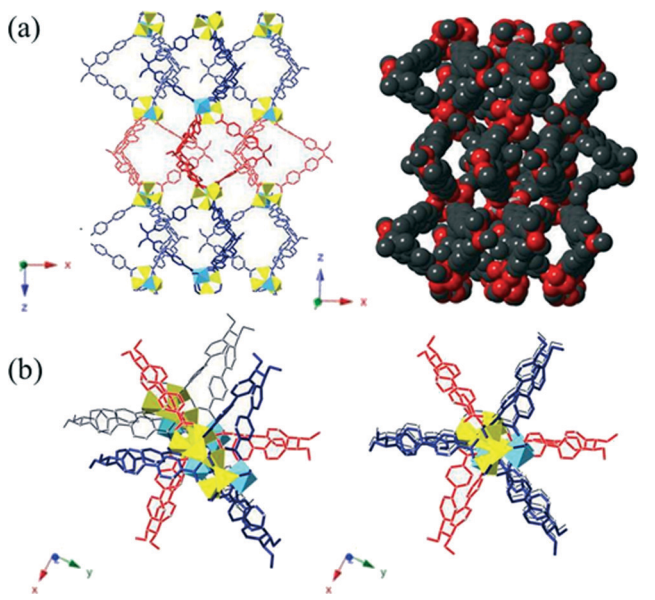

Fig. 3 (a) Side view of Zn-(+)-**2** along the *b* axis. (b) Left: view of two rods in Zn-(+)-**2** along the *c* axis, with one rod in red and blue, the other one in grey. Right: view of one rod only.

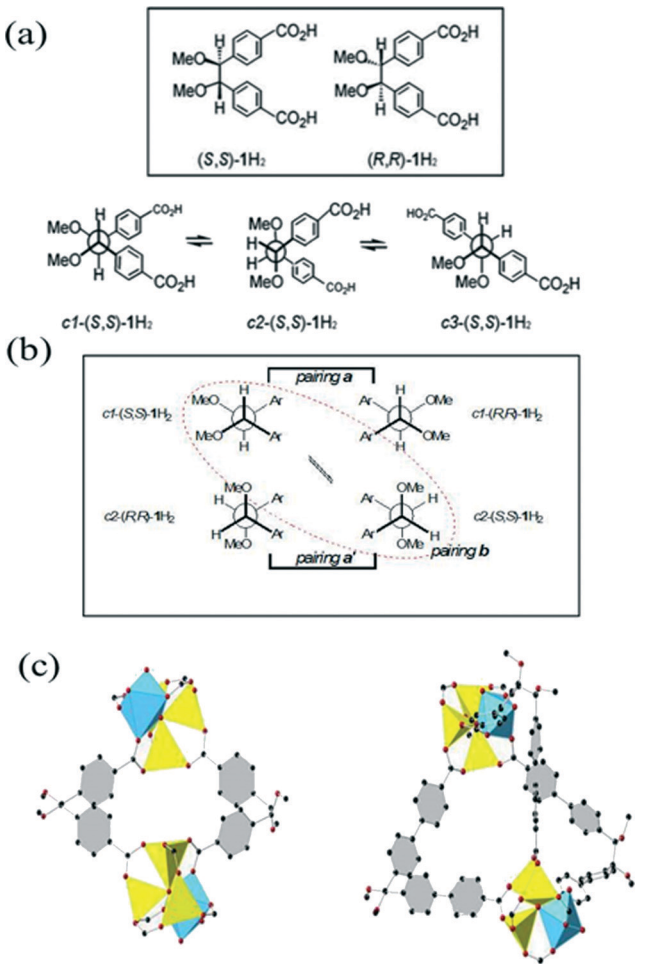

Fig. 4 (a) Enantiomers of $\mathbf{1}H_2$ ligands and their energy minimum staggered conformers. (b) Newman projections of the conformers of $\mathbf{1}H_2$ and their pairings, with pairing b found in the structure of Zn-(+)-**1**. (c) Asymmetric units for Zn-(+)-**1** and Zn-(+)-**2**.

not unusual. This was accounted for by the strong tendency of adopting the centrosymmetric (or *pseudo*centrosymmetric) arrangement in the asymmetric units of the supramolecules even obtained from components with chirality.[12] Since ligands $1H_2$ and $2H_2$ have flexible ethylene bridges between the two aromatic carboxylates, they could have three major conformers with staggered arrangements, as shown in Fig. 4a for $1H_2$. A close investigation of the ligands in Zn-(+)-**1** reveals that the small squares are formed by the pairing of two inter-convertible conformers of bent struts, c1 and c2, to imitate the centrosymmetric asymmetric unit, as already seen in the case of La-(+)-**1**.[12e] With emphasis on the aromatic backbone, it was apparent that c2-(*S*,*S*)-**1** exhibited a close similarity to c1-(*R*,*R*)-**1**. Thus, c2-(*S*,*S*)-**1** disguised itself as c1-(*R*,*R*)-**1** and produced a near-centrosymmetric local unit by pairing with c1-(*S*,*S*)-**1**. On the other hand, in Zn-(+)-**2**, supermolecular building blocks containing *pseudo*-centrosymmetric units could be assembled from single conformers like c1-(*S*,*S*)-**2** (Fig. 4c), leading to the chirality mitigation as observed in similar cyclodextrin systems.[11]

Acknowledgements

The authors are grateful to Professor Jaheon Kim (Soongsil University) for his help in refinement of the crystal structures and valuable comments. The financial support from the Korean government through the NRF (NRF-2011-0016303), National Natural Science Foundation of China (21101030), and Creative Research Group of MOE (IRT1117) is appreciated. Experiments at PLS (beamline 2D-SMC, 2012-3rd-2D-016) were supported in part by MEST and POSTECH.

Notes and references

‡ Crystallographic data for Zn-(+)-**1**: $C_{317}H_{352}N_{21}O_{105}Zn_{16}$, M_r = 7182.12, triclinic, space group *P*1 (no. 1), crystal size 0.20 × 0.20 × 0.05 mm^3, T = 258(2) K, a = 21.701(4) Å, b = 23.071(5) Å, c = 23.286(5) Å, α = 63.91(3)°, β = 38.86(3)°, γ = 64.98(3)°, V = 9264(3) $Å^3$, Z = 1, d_{calc} = 1.287 g m^{-3}, λ = 1.54178 Å, R_1 = 0.0710 ($I > 2\sigma(I)$), wR_2 = 0.2124 (all data), GOF = 0.982, the Flack's x parameter = 0.02(2), 34 979 independent reflections (2θ = 58.82°), and 2231 parameters; crystallographic data for Zn-(+)-**2**: $(Zn_4O)_2(2)_6(DEF)_4$ = $C_{200}H_{188}N_4O_{42}Zn_8$, M_r = 3842.50, orthorhombic, space group $P2_12_12_1$ (no. 19), crystal size 0.12 × 0.05 × 0.04 mm^3, T = 100(2) K, a = 22.945(5) Å, b = 31.803(6) Å, c = 32.955(7) Å, V = 24 048(8) $Å^3$, Z = 4, d_{calc} = 1.061 g m^{-3}, μ (λ = 0.9000Å) = 1.569 mm^{-1}. R_1 = 0.0788, wR_2 = 0.2107 ($I > 2\sigma(I)$), R_1 = 0.1115, wR_2 = 0.1906 (all data), GOF = 0.927, the Flack's x parameter = 0.052(13), 26 210 independent reflections (2θ = 27.5°), and 2273 parameters; CCDC reference numbers for Zn-(+)-**1**: 848661 and Zn-(+)-**2**: 834932.

1 (*a*) O. M. Yaghi, M. O'Keeffe, N. W. Ockwig, H. K. Chae, M. Eddaoudi and J. Kim, *Nature*, 2003, **423**, 705; (*b*) S. Kitagawa, R. Kitaura and S. Noro, *Angew. Chem., Int. Ed.*, 2004, **43**, 2334; (*c*) G. Férey, *Chem. Soc. Rev.*, 2008, **37**, 191; (*d*) A. U. Czaja, N. Trukhan and U. Müller, *Chem. Soc. Rev.*, 2009, **38**, 1284.

2 Q. Li, W. Zhang, O. Š. Miljanić, C.-H. Sue, Y.-L. Zhao, L. Liu, C. B. Knobler, J. F. Stoddart and O. M. Yaghi, *Science*, 2009, **325**, 855.

3 (*a*) R. B. Getman, Y.-S. Bae, C. E. Wilmer and R. Q. Snurr, *Chem. Rev.*, 2012, **112**, 703; (*b*) K. Sumida, D. L. Rogow, J. A. Mason, T. M. Mcdonald, E. D. Bloch, Z. R. Herm, T.-H. Bae and J. R. Long, *Chem. Rev.*, 2012, **112**, 724; (*c*) M. P. Suh, H. J. Park, T. K. Prasad and D.-W. Lim, *Chem. Rev.*, 2012, **112**, 782; (*d*) H. Wu, Q. Gong, D. H. Olson and J. Li, *Chem. Rev.*, 2012, **112**, 836; (*e*) H. Li, M. Eddaouddi, T. L. Groy and O. M. Yaghi, *J. Am. Chem. Soc.*, 1998, **120**, 8571; (*f*) N. Rosi, J. Eckert, M. Eddaoudi, D. Vodak, J. Kim, M. O'Keeffe and O. M. Yaghi, *Science*, 2003, **300**, 1127.

4 (*a*) J.-R. Li, J. Sculley and H.-C. Zhou, *Chem. Rev.*, 2012, **112**, 869; (*b*) J.-R. Li, R. J. Kuppler and H.-C. Zhou, *Chem. Soc. Rev.*, 2009, **38**, 1477; (*c*) M. E. Davis, *Nature*, 2002, **417**, 813.

5 (*a*) M. Yoon, R. Srirambalaji and K. Kim, *Chem. Rev.*, 2012, **112**, 1196; (*b*) K. S. Jeong, Y. B. Go, S. M. Shin, S. J. Lee, J. Kim, O. M. Yaghi and N. Jeong, *Chem. Sci.*, 2011, **2**, 877; (*c*) L. Ma, J. M. Falkowski, C. Abney and W. Lin, *Nat. Chem.*, 2010, **2**, 838; (*d*) L. Ma, C. Wang, J. M. Falkowski, L. Ma and W. Lin, *J. Am. Chem. Soc.*, 2010, **132**, 15390; (*e*) D. Dang, P. Wu, C. He, Z. Xie and C. Duan, *J. Am. Chem. Soc.*, 2010, **132**, 14321.

6 (*a*) R. E. Morris and X. Bu, *Nat. Chem.*, 2010, **2**, 353; (*b*) C. J. Kepert, T. J. Prior and M. J. Rosseinsky, *J. Am. Chem. Soc.*, 2000, **122**, 5158; (*c*) D. Bradshaw, T. J. Prior, E. J. Cussen, J. B. Claridge and M. J. Rosseinsky, *J. Am. Chem. Soc.*, 2004, **126**, 6106; (*d*) Z. Lin, A. M. Z. Slawin and R. E. Morris, *J. Am. Chem. Soc.*, 2007, **129**, 4880; (*e*) J. Zhang, S. Chen, T. Wu, P. Feng and X. Bu, *J. Am. Chem. Soc.*, 2008, **130**, 12882.

7 M. O'Keeffe, M. A. Peskov, S. J. Ramsden and O. M. Yaghi, *Acc. Chem. Res.*, 2008, **41**, 1782.

8 (*a*) T. M. Reineke, M. Eddaoudi, D. Moler, M. O'Keeffe and O. M. Yaghi, *J. Am. Chem. Soc.*, 2000, **122**, 4843; (*b*) H. M. El-Kaderi, J. R. Hunt, J. L. Mendoza-Cortés, A. P. Côté, R. E. Taylor, M. O'Keeffe and O. M. Yaghi, *Science*, 2007, **316**, 268.

9 S. H. Cho, B. Q. Ma, S. T. Nguyen, J. T. Hupp and T. E. Albrecht- Schmitt, *Chem. Commun.*, 2006, 2563.

10 D. Zhao, D. J. Timmons, D. Yuan and H.-C. Zhou, *Acc. Chem. Res.*, 2011, **44**, 123.

11 (*a*) K. Kano, *J. Phys. Org. Chem.*, 1997, **10**, 286; (*b*) K. Kano and R. Nishiyabu, *J. Inclusion Phenom. Macrocyclic Chem.*, 2003, **44**, 355; (*c*) K. Kano and R. Nishiyabu, in *Advances in Supramolecular Chemistry*, ed. G. W. Gokel, Cerberus Press, Inc., South Miami, FL, USA, 2003, vol. 9, pp. 39–69.

12 (*a*) K. S. Jeong, Y. S. Kim, Y. J. Kim, E. Lee, J. H. Yoon, W. H. Park, Y. W. Park, S.-J. Jeon, Z. H. Kim, J. Kim and N. Jeong, *Angew. Chem., Int. Ed.*, 2006, **45**, 8134; (*b*) K. S. Jeong, S. Y. Kim, Y. Oh, D. W. Min, J. Kim and N. Jeong, *CrystEngComm*, 2007, **9**, 273; (*c*) K. S. Jeong, B. H. Lee, J. Kim and N. Jeong, *CrystEngComm*, 2009, **11**, 549; (*d*) K. S. Jeong, D. E. Kim, E. Lee, Y. H. Jhon, H. Han and N. Jeong, *Tetrahedron: Asymmetry*, 2009, **20**, 1736; (*e*) K. S. Jeong, B. H. Lee, Q. Li, S. B. Choi, J. Kim and N. Jeong, *CrystEngComm*, 2011, **13**, 1277.

